

TIME STEP DEPENDENCE IN THE PREDICTION OF FLOW DYNAMICS IN AN INTERNAL COMBUSTION ENGINE

Charles Rech, charlesrech@uol.com.br

Mechanical Engineering Department, Lutheran University of Brazil

Flavio V Zancanaro Jr., zancanaro@mecanica.ufrgs.br

Mechanical Engineering Graduate Program, Federal University of Rio Grande do Sul, Brazil

Horácio A Vielmo, vielmoh@mecanica.ufrgs.br

Mechanical Engineering Department, Federal University of Rio Grande do Sul, Brazil

Abstract. *This paper discusses the time step dependence in the prediction of transient flow in an internal combustion engine, under the motored condition. The parameter considered was the discharge coefficient in the maximum piston velocity, at 75° after Top Dead Center (aTDC). The time steps considered for the study were: 5°, 1°, 0.5°, 0.2°, 0.1°, 0.05°, 0.01°, 0.005° of the crank angle (CA). The transient flow that occurs in the intake system and in-cylinder were investigated in a standard CFR (Cooperative Fuel Research) engine, with bore of 82.55 mm and a stroke of 114.30 mm. The three-dimensional modeling includes a flat piston, intake and exhaust conventional type and valves and piston movements with angular speed of 200 rpm. Numerical solutions using a Commercial Finite Volumes CFD code are performed, applying moving unstructured hexahedral-trimmed mesh, using parallel computation. Regarding turbulence, computations were performed with Reynolds-Averaged Navier-Stokes, Eddy Viscosity Model $k-\omega$ SST, in its Low-Reynolds approach with hybrid near wall treatment. Convergence tests were performed and a secure criterion established. The enthalpy equation is also solved and the air is treated as a perfect gas, taking compressibility into account. A mesh independence study was performed, through discharge coefficient in the maximum piston velocity.*

Keywords: *Time step dependence, CFD, moving mesh*

1. INTRODUCTION

In internal combustion engines (ICE), the flow conditions inside the cylinder are critical for the combustion process (Heywood, 1988). These are determined by the air flowing into the cylinder through the intake valves during the induction process and by its evolution during the compression stroke.

There are many techniques to analyze the flow into the cylinder from experimental measures, for example the measurement of the velocity field in the steady flow test rig using laser Doppler velocimetry (Uzkan *et al.*, 1983). This method provides high quality results and is more aptly used to measure the velocity field inside the cylinder while the engine is working, although this requires expensive equipment and good optical access to the combustion chamber (Zur *et al.*, 1989, Payri *et al.*, 1996, Rask *et al.*, 1985, Jaffri *et al.*, 1997, Fansler *et al.*, 1993, Corcione *et al.*, 1994, Bopp *et al.*, 1986).

Another approach for gaining insight into the in-cylinder flow is the application of three-dimensional calculation codes, which are able to solve the governing flow equations, and thus yield detailed descriptions of the mean velocity and the turbulent velocity fields (Bianchi *et al.*, 2002, Baratta *et al.*, 2008a, Baratta *et al.*, 2008b, Zancanaro *et al.*, 2010, Zancanaro, 2010, Rech *et al.*, 2010).

With the exponentially increasing computational power of modern computers, multi-dimensional Computational Fluid Dynamics (CFD) has found more and more applications in internal combustion engines research, design and development. Enhanced understandings of the physical processes of combustion and correspondingly improved numerical models and methods have both driven multi-dimensional CFD simulation tools from qualitative description towards quantitative prediction (Lakshminarayanan and Aghav, 2010). Therefore, powerful CFD codes are required to have the capability of predicting complex turbulent flows from engine developments and design in a reasonable time scale.

In this work, are showed the results for the discharge coefficient at 75° for time step 5°, 1°, 0.5°, 0.2°, 0.1°, 0.05°, 0.01°, 0.005° of the crank angle in a CFR engine. The results were obtained by the numerical solutions using a commercial Finite. For both parameters were observed the dependence of the results at time step employed.

2. CASE DESCRIPTON

The engine under investigation is of a single cylinder four-stroke motored CFR engine (Fig. 1). The specifications of the engine are given in the Table 1.

Table 1. Specifications of the CFR engine

ASTM-CFR - engine	
Bore (B)	82.55 mm
Stroke	114.30 mm
Intake Valve Open (IVO)	0°
Intake Valve Close (IVC)	202°
Displacement	611.30 cm ³
Maximum valve lift	6.05 mm
Intake air system	Naturally aspirated
Compression ratio	6:1
Speed (N)	200 rpm



Figure 1 – CFR engine

3. MATHEMATICAL MODEL

The velocity field is described by the mass and momentum conservation equations (Navier-Stokes), in their transient, compressible form.

In Cartesian tensor notation, according Warsi (1981), the mass conservation is

$$\frac{\partial \rho}{\partial t} + \frac{\partial}{\partial x_j} (\rho u_j) = 0 \quad (1)$$

and the momentum

$$\frac{\partial \rho u_i}{\partial t} + \frac{\partial}{\partial x_j} (\rho u_j u_i - \tau_{ij}) = -\frac{\partial p}{\partial x_i} + s_i \quad (2)$$

being p the piezometric pressure defined:

$$p = p_s - \rho_0 g_m x_m \quad (3)$$

where p_s is static pressure, ρ_0 is reference density, g_m the are gravitational acceleration components and the x_m are coordinates relative to a datum where ρ_0 is defined.

As the fluid is Newtonian, and the flow is turbulent, assuming the ensemble average (equivalent to time averages for steady-state situations), the stress tensor components are, according Hinze (1975),

$$\tau_{ij} = 2\mu s_{ij} - \frac{2}{3}\mu \frac{\partial u_k}{\partial x_k} \delta_{ij} - \overline{\rho u'_i u'_j} \quad (4)$$

and strain tensor

$$s_{ij} = \frac{1}{2} \left(\frac{\partial u_i}{\partial x_j} + \frac{\partial u_j}{\partial x_i} \right) \quad (5)$$

The u' are fluctuations about the ensemble average velocity, and overbar denotes the ensemble averaging process. Finally, as the flow is compressible and non-isothermal, in the Eq. (2)

$$s_i = g_i (\rho - \rho_0) \quad (6)$$

where g_i is the gravitational acceleration component in x_i direction. Considering the air as an ideal gas

$$\rho = \frac{P}{RT} \quad (7)$$

For the heat transfer problem, the enthalpy equation is also solved. According Jones (1980),

$$\frac{\partial \rho h}{\partial t} + \frac{\partial}{\partial x_j} (\rho h u_j + F_{h,j}) = \frac{\partial p}{\partial t} + u_j \frac{\partial p}{\partial x_j} + \tau_{ij} \frac{\partial u_i}{\partial x_j} \quad (8)$$

where $h = \bar{c}_p T - c_p^0 T_0$ is the static enthalpy; \bar{c}_p is the mean constant-pressure specific heat at temperature T ; c_p^0 the reference specific heat at temperature T_0 , and $F_{h,j}$ the diffusional energy flux in direction x_j , given by

$$F_{h,j} \equiv -k_t \frac{\partial T}{\partial x_j} + \bar{\rho} \overline{u'_i h'} \quad (9)$$

where k_t is the thermal conductivity.

2.1 Constitutive Relations

The rightmost terms of the Eq. (4) and Eq. (9) represents the additional Reynolds stresses due to turbulent motion. These are linked to the mean velocity field via turbulence models. According Launder and Spalding (1974), for linear viscosity models

$$-\bar{\rho} \overline{u'_i u'_j} = u_i S_{ij} - \frac{2}{3} \left(u_i \frac{\partial u_k}{\partial x_k} + \rho k \right) \delta_{ij} \quad (10)$$

and

$$-\bar{\rho} \overline{u'_i h'} = -\frac{\mu_t}{\sigma_{h,t}} \frac{\partial h}{\partial x_j} \quad (11)$$

where $k = \overline{u'_i u'_i} / 2$ is the turbulence kinetic energy; μ_t the turbulent viscosity; $\sigma_{h,t}$ the turbulent Prandtl number and mean strain is

$$S_{ij} = \frac{\partial u_i}{\partial x_j} + \frac{\partial u_j}{\partial x_i} \quad (12)$$

2.2 Governing Equations for the SST k - ω Turbulence Model

The specific dissipation rate is defined as $\omega = \varepsilon / C_\mu k$, and the general form of the turbulent kinetic energy is

$$\frac{\partial}{\partial t} (\rho k) + \frac{\partial}{\partial x_j} \left[\rho u_j k - \left(\mu + \frac{\mu_t}{\sigma_k^\omega} \right) \frac{\partial k}{\partial x_j} \right] = \mu_t P - \rho \beta^* k \omega + \mu_t P_B \quad (13)$$

and specific dissipation rate is

$$\frac{\partial}{\partial t} (\rho \omega) + \frac{\partial}{\partial x_j} \left[\rho u_j \omega - \left(\mu + \frac{\mu_t}{\sigma_\omega^\omega} \right) \frac{\partial \omega}{\partial x_j} \right] = \alpha \frac{\omega}{k} \mu_t P - \rho \beta \omega^2 + \rho S_\omega + C_{\varepsilon 3} \mu_t P_B C_\mu \omega \quad (14)$$

being

$$P \equiv S_{ij} \frac{\partial u_i}{\partial x_j} \quad ; \quad P_B \equiv -\frac{g_i}{\sigma_{h,t}} \frac{1}{\rho} \frac{\partial \rho}{\partial x_i} \quad (15)$$

and C_{e3} and C_μ are empirical coefficients. For $k-\omega$ SST model, the other coefficients are given in Menter (1993). In the SST $k-\omega$ model the turbulent viscosity is linked to k and ω via

$$\mu_t = \frac{a_1 k}{\max\left(a_1 \omega, \sqrt{\frac{1}{2} \Omega_{ij} \Omega_{ij}} F_2\right)} \quad (16)$$

3. NUMERICAL METHODOLOGY

Numerical transient solutions using the commercial Finite Volumes CFD code StarCD es-ice were performed, for a CFR engine. A user defined unstructured hexahedral-trimmed cells moving mesh was constructed, as showed in the Fig. 2 and Fig 3. A mesh independence study was performed, arriving in 660813 cells in the domain (Fig. 4). Regarding the turbulence, it is applied the $k-\omega$ SST model in Low-Reynolds approach, with hybrid near wall treatment. All computations were performed with double precision. The pressure-velocity coupling is solved through the SIMPLE algorithm with 1×10^{-4} residual for all variables. The used differencing scheme is the Linear Upwind Differencing (LUD), with blending factor (bf) of 0.5 for the momentum, turbulence and enthalpy equations and $bf = 0.1$ for pressure. For the density, the Central Differencing (CD), with $bf = 0.5$, was applied.

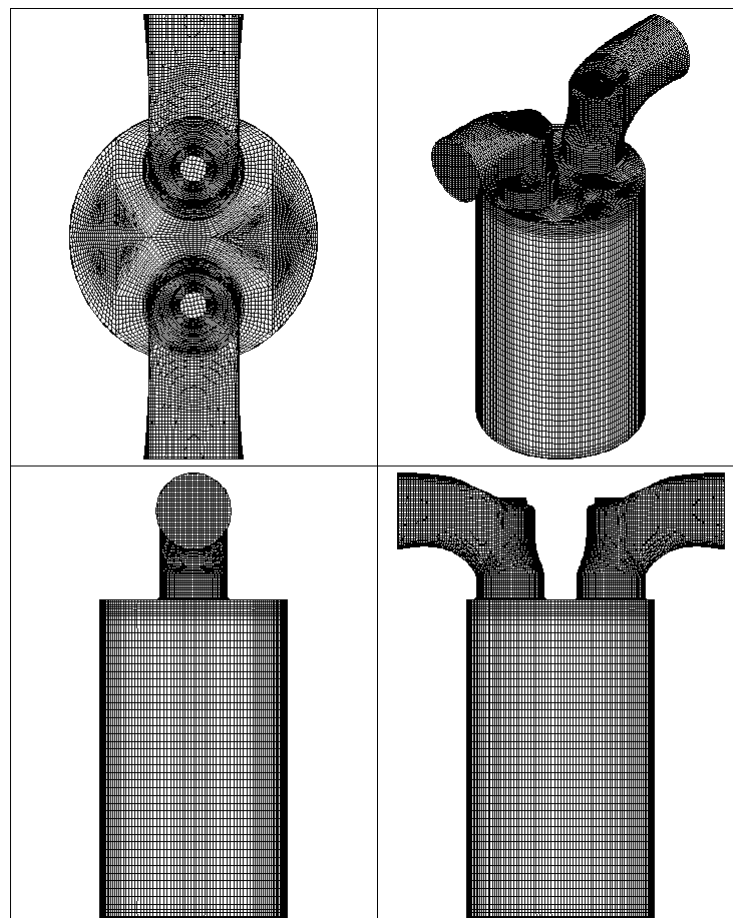


Figure 2 - Unstructured hexahedral-trimmed cells moving mesh

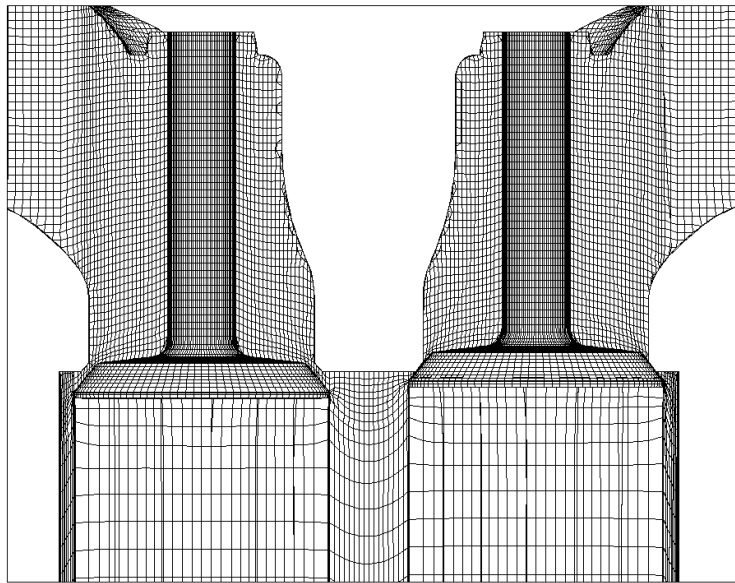


Figure 3 –Unstructured hexahedral-trimmed cells moving mesh detail

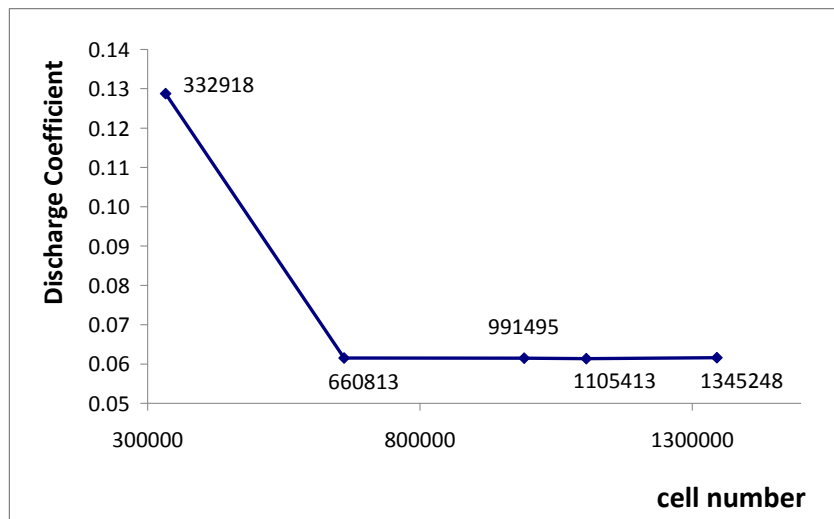


Figure 4 - Mesh independence study for the maximum piston velocity, at 75° aTDC

3.1 Boundary and Initial Conditions

The boundary conditions are stagnation pressure (p_{st}) of 1 atm at the inlet, with 293.15 K, discharging in an ambient pressure (p_{out}) of 1 atm, and 293.15 K. For all cases the turbulence boundary conditions are turbulence intensity $I = 0.05$, and length scale $l = 0.0034$ m, as a consequence of the flow and geometrical characteristics. Regarding the heat transfer problem, considering a cold flow (exhaust and compression processes, without combustion), the cylinder wall and piston crown have a constant temperature of 400 K, and a thermal resistance of $0.004 \text{ m}^2\text{K/W}$. Accordingly, for the combustion chamber dome, values are 450 K and $0.004 \text{ m}^2\text{K/W}$. For intake and exhaust valves and ports the temperature is 350 K and thermal resistance is $0.004 \text{ m}^2\text{K/W}$.

As initial condition for the independency mesh analysis, the crankshaft starts at 360°, almost at the end of the exhaust process. All the velocity components inside the cylinder are set to 0.1 m/s, at 1 atm and 300 K. For the rest of the simulation, the initial conditions are the final values of the previous cycle.

4. EXPERIMENTAL METHODOLOGY

To experimental date the engine was instrumented with data acquisition, angular position and air flow measurement. The angular position of the crankshaft was measured with an incremental encoder (Danaher Sensors & Controls, model BA 3022). The encoder was connected to the crankshaft and supplied 1733.33 pulses per revolution, with a resolution of 0.20769 degrees. The mass air flow was measured with an automotive hot film anemometer. (MAF -Bosch 0 280 218 002). The data was acquired with a commercial data acquisition board (National instruments 6124) and its original software LabView. The values of voltage and frequency were collected and processed with the correspondent calibration curves of each sensor and converted into units of mass flow and angular position. It was acquired 6000 samples for second (Rech *et al.*, 2010).

5. THE DISCHARGE COEFFICIENT (C_{D_actual})

The impact of a blockage on engine breathing is assessed through a discharge coefficient C_D that relates the actual mass flow rate through the intake valve to the isentropic mass flow rate. Therefore, the equation assumes the following form (Heywood, 1988; Ferrari, 2005).

$$C_{D_actual} = \frac{\dot{m}_{actual}}{\frac{\pi d_v^2}{4} \frac{p_{st}}{(RT_o)^{1/2}} \left(\frac{p_{out}}{p_{st}}\right)^{1/\gamma} \left\{ \frac{2\gamma}{\gamma-1} \left[1 - \left(\frac{p_{out}}{p_{st}}\right)^{(\gamma-1)/\gamma} \right] \right\}^{1/2}} \quad (17)$$

where \dot{m}_{actual} is obtained from the numerical solution, or experimentally, R is the gas (air) constant, T_o the stagnation (inlet) absolute temperature, d_v is the inner valve diameter and γ the specific heat ratio.

6. RESULTS AND DISCUSSION

The above mentioned model has been implemented in the StarCD es-ice. Results from StarCD es-ice code will be compared with experimental measurements. Details of the complex flow generated in the intake stroke for several time steps are presented and discussed. The used numerical methodology was verified and presented in another work (Rech *et al.*, 2010).

The Table 2 shows the results for the discharge coefficient at 75° aTDC, in the maximum piston velocity. Better agreement between model and experimental measurements can be achieved for the smallest time step, but this situation requires large computational effort and becoming unviable without the use of parallel computational.

Table 2. Comparative parameters at 75° aTDC

Time Step [°]	Discharge Coefficient (C_{D_actual})
0.005	0.062537
0.01	0.062415
0.05	0.062366
0.1	0.062349
0.2	0.062335
0.5	0.062229
1	0.061412
5	0.059072
Experimental	0.064103

The Fig. 5a shows the results for the discharge coefficient as a function of the crank angle to time steps from 0° until 35°. In this interval, only the time steps of 0.2° to 0.005° had revealed good agreement among the obtained results. The another time steps (0.5°_5°) showed minor agreement, so, is possible that this time steps are not adjusted to predict the coefficient of discharge, considering the used numerical parameters in engine CFR. The Fig. 5b shows the results for the discharge coefficient as a function of the crank angle to time steps from 35° until 75°. It is verified that from 35° aTDC the results are in the same band, and have good agreement with experimental results presented in the Table 1 and by the authors in another work (Rech *et al.*, 2010), except for the time step of 1°, 2.5° and 5°.

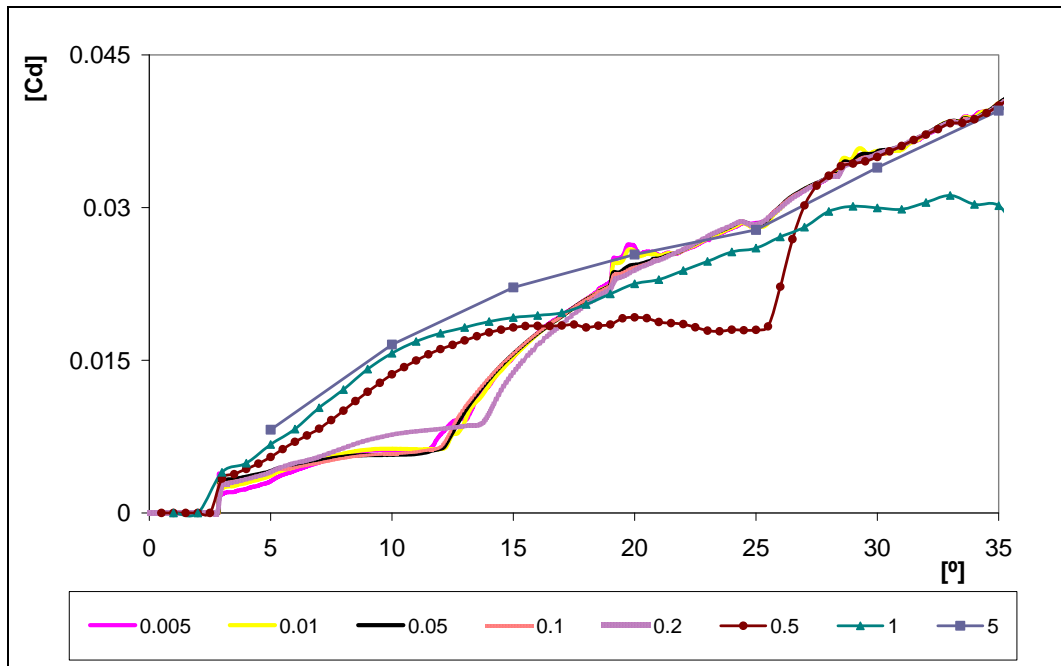


Figure 5a. Evolution of the discharge coefficient as a function of the crank angle to time steps from 0° until 35°

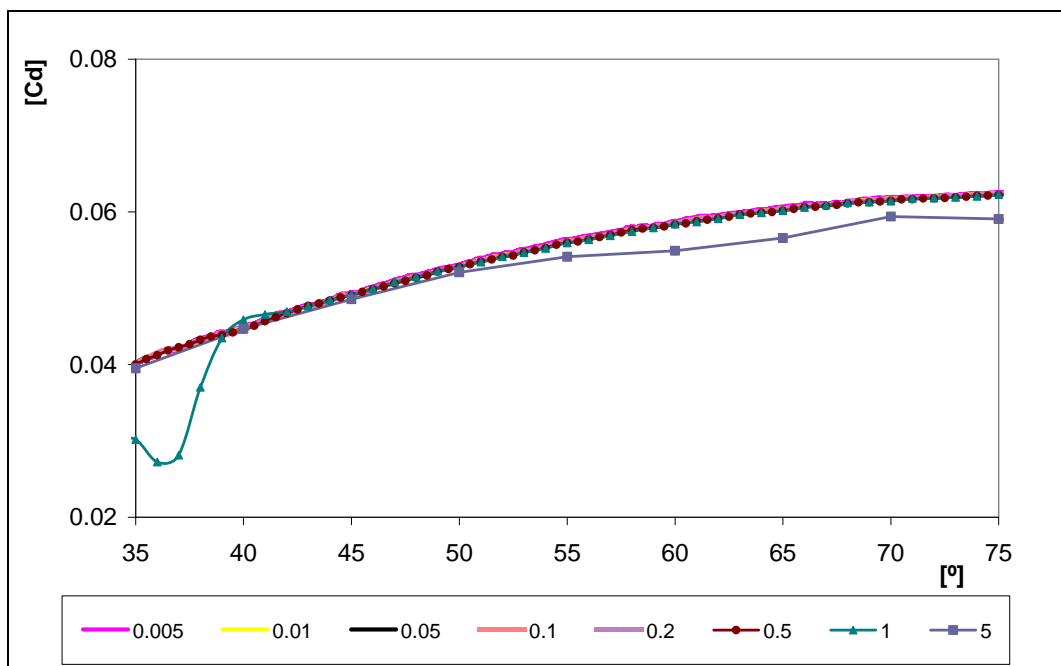


Figure 5b. Discharge coefficient as a function of the crank angle to time steps from 35° until 75°

7. CONCLUSION

In order to predict the time step dependence in the solution in-cylinder flow field of a CFR engine, numerical methodology were employed for studying the 3D turbulent transient compressible flow at 200 rpm. Comparisons were made for time step dependence considering discharge coefficient.

The results for the maximum piston velocity (75° aTDC) showed good agreement among all time step studied, with an exception for the biggest one (5°). By the other way, before 35°, only 0.005° to 0.2° time steps present a good agreement. In this case, the results for the time steps 0.5° to 5° are not representative of the discharge coefficient.

Finally, it can be concluded that the early moment of the intake process, when the intake valve is in the beginning of its lift, the numerical simulation presents its major challenge.

8. ACKNOWLEDGEMENTS

The authors thank the financial support from CNPq, Brazil, through a doctoral grant to Zancanaro, F V Jr, scientific productivity grant to Vielmo, H A. and the Universal Project 475237/2009-9. Also, the authors would like to thank the CESUP/UFRGS, RS, Brazil.

9. REFERENCES

- Baratta, M.; Catania, A.E.; Pesce, F.C.; Spessa, E.; Rech C.; Vielmo, H.A., 2008a “Multidimensional Modeling of a High Swirl-Generating Helical Intake Port for Diesel Engines”, 12th Brazilian Congress of Thermal Engineering and Sciences, Belo Horizonte -MG, Proceedings of ENCIT, Rio de Janeiro, RJ: ABCM.
- Baratta, M.; Catania, A.E.; Pesce, F.C.; Spessa, E.; Rech, C.; Vielmo, H.A., 2008b “Comparisons Between Steady State Analyses of a High Swirl-Generating Helical Intake Port for Diesel Engines”, 12th Brazilian Congress of Thermal Engineering and Sciences, Belo Horizonte - MG. Proceedings of ENCIT, Rio de Janeiro, RJ: ABCM.
- Bianchi, G.M.; Cantore, G.; Fontanesi, S., 2002 “Turbulence Modeling in CFD Simulation of ICE Intake Flows: The Discharge Coefficient Prediction”, SAE Paper No 2002-01-1118.
- Bopp S, Vafidis C, Whitelaw JH., 1986 “The effect of engine speed on the TDC flowfield in a motored reciprocating Engine”. SAE 860023.
- Corcione FE, Valentino G., 1994 “Analysis of in-cylinder flow processes by LDA”. *Combust Flame*;99:387–94.
- Fansler T.D., 1993 “Turbulence production and relaxation in bowl-in-piston engines”. SAE 930479.
- Ferrari, G., 2005, “Motori a Combustione Interna”, Torino, Ed il Capitello, (in italian).
- Heywood, J.B., 1988, "Internal Combustion Engines", McGraw-Hill Inc.
- Hinze, P.O., 1975, “Turbulence”, 2nd Edition, McGraw-Hill, New York.
- Jaffri K, Hascher HG, Novak M, Lee K, Schock H, Bonne M, et al., 1997 “Tumble and swirl quantification within a motored four-valve SI engine cylinder based on 3-D LDV measurements”. SAE 970792.
- Launder, B.E. and Spalding, D.B., 1974 “The Numerical Computation of Turbulent Flows, Computational Methods in Applied Mechanics and Engineering”, 3, pp. 269-289.
- Menter, F.R., 1993 “Zonal Two Equation $k-\omega$ Turbulence Models for Aerodynamic Flows” Proc. 24th Fluid Dynamics Conf., Orlando, Florida, USA, Paper No. AIAA 93-2906.
- Payri F, Desantes JM, Pastor JV., 1996 “LDV measurements of the flow inside the combustion chamber of a 4-valve D.I. Diesel engine with axisymmetric piston bowls”. *Experiments in Fluids*; Vol. 22:118–28.
- Rask RB, Saxena V., 1985 “Influence of the geometry on flow in the combustion chamber of a direct-injection Diesel Engine”. ASME Winter Annual Meeting. p. 19–28.
- Rech, C, Zancanaro, F V Jr, Wildner, F. D., Vielmo, H.A., Oliveira A. M. Jr., 2010 “Experimental and Numerical Analysis of Gas Motion in a Standard Cooperative Fuel Research Engine”, 13th Brazilian Congress of Thermal Engineering and Sciences, Uberlândia - MG. Proceedings of ENCIT, Rio de Janeiro, RJ: ABCM.
- StarCD Version 4.10. Methodology, CD-adapco, 2009.
- Uzkan T, Borgnakke C, Morel T., 1986, “Characterization of flow produced by a high-swirl inlet port” SAE Paper 830266.
- Warsi, Z.V.A., 1981, “Conservation Form of the Navier-Stokes Equations in General Nonsteady Coordinates”, *AIAA Journal*, 19, pp. 240-242.
- Zancanaro, F. V. Jr., 2010a “Simulação Numérica do Escoamento Turbulento em Motores de Combustão Interna”, Porto Alegre, UFRGS, Dissertação de mestrado.
- Zancanaro, F. V. Jr., Vielmo, H.A., 2010 “Intake Flow and Time Step Analysis in the Modeling of a Direct Injection Diesel Engine”, 13th Brazilian Congress of Thermal Engineering and Sciences, Uberlândia - MG. Proceedings of ENCIT, Rio de Janeiro, RJ: ABCM.
- Zur Loye AO, Siebers DL, Mckinley TL, Ng HK, Primus RJ., 1989, “Cycle-resolved LDV measurements in a motored Diesel engine and comparison with $k-\epsilon$ model predictions” SAE 890618.

11. RESPONSIBILITY NOTICE

The authors are the only responsible for the printed material included in this paper.